Reflection Absorption Infrared Spectroscopy and Temperature-Programmed Desorption Studies of the Adsorption and Desorption of Amorphous and Crystalline Water on a Graphite Surface

Amandeep S. Bolina, Angela J. Wolff, and Wendy A. Brown*

Department of Chemistry, University College London, 20 Gordon Street, London, WC1H 0AJ, U.K.

Received: May 27, 2005; In Final Form: July 12, 2005

Reflection absorption infrared spectroscopy (RAIRS) and temperature-programmed desorption (TPD) have been used to perform a detailed investigation of the adsorption of water on highly oriented pyrolytic graphite (HOPG) at 90 K. RAIRS shows that water is physisorbed on HOPG at all coverages, as expected. Experiments at higher surface temperatures show marked changes in the O−H stretching region of the spectrum which can be assigned to the observation of the amorphous to crystalline ice phase transition. The infrared signature of both phases of solid water has been determined on HOPG and can be used to identify the phase of the ice. TPD spectra show the desorption of multilayers of crystalline ice. At high exposures a small bump appears in the TPD spectrum, on the low temperature side of the main peak, which is attributed to the amorphous to crystalline phase transition. At very low exposures of water, it is possible to distinguish the desorption of water from two- and three-dimensional islands and hence to determine the growth mode of water on the HOPG surface. Isothermal TPD studies have also been performed and show that the desorption of water does not obey perfect zero-order kinetics. Desorption orders, derived directly from the TPD spectra, confirm this observation. Desorption energies and preexponential factors have also been determined for this adsorption system.

Introduction

Water (H_2O) is found in the interstellar medium (ISM) in the form of interstellar ices, frozen out on the surface of dust grains.[1] Water accounts for 60−70% of the composition of these ices[2,3] and hence plays a significant role in the chemistry of the ISM. A clear understanding of the adsorption and desorption of water from dust grain surfaces is therefore crucial in understanding gas−grain interactions and, in turn, the chemistry of interstellar space. Furthermore, it has been shown that the desorption of all species accreted on dust grains, such as methanol, carbon dioxide, and ammonia, is controlled by the behavior of water ice.[4] With this in mind, we have used reflection absorption infrared spectroscopy (RAIRS) and temperature-programmed desorption (TPD) to perform a detailed investigation of the adsorption of water on, and its desorption from, a highly oriented pyrolytic graphite (HOPG) surface held at around 90 K.

Dust grains in the ISM consist mainly of carbonaceous and silicaceous material and are often covered in films of ice.[1] HOPG, and other carbon based surfaces, can be considered suitable analogues of dust grains and have been used previously in investigations of H_2 formation on dust grain surfaces.[5−8] The temperature in the ISM, where these ice-covered grains are found, is around 10−20 K. Although the experiments described here are not undertaken at this temperature, they still allow an understanding of the interaction of water with the HOPG surface to be gained. In fact, previous studies of the desorption of water ice from a Au surface[4] have shown that desorption does not occur at temperatures below 100 K.

Because of its importance in a variety of areas, water adsorption on surfaces has received much attention. Thorough reviews of the fundamental interactions of water with solid surfaces (mainly metals) have been presented by Henderson[9] and by Thiel and Madey.[10] There have also been several previous studies of the adsorption of water on graphitic surfaces. Phelps and co-workers investigated the adsorption of water on HOPG at 88 K using high-resolution electron energy loss spectroscopy (HREELS).[11] Loss features were observed at 235, 735, and 3340 cm^{-1}, along with a weak feature at 1600 cm^{-1}. The frequencies of the adsorbate peaks were independent of the water exposure, indicating that physisorption occurred at all coverages. Water adsorption was found to be associative, with the adlayer forming hydrogen bonded clusters.[11]

Similar findings were reported in a HREELS study of water adsorbed on HOPG at 85 K by Chakarov and co-workers.[12,13] Loss features, typical of condensed water ice, were noted at 200 cm^{-1} (frustrated translation), 710 cm^{-1} (frustrated rotation), 1595 cm^{-1} (HOH scissors mode), and 3345 cm^{-1} (symmetric stretch). Chakarov also investigated the adsorption of water on HOPG using TPD.[12,13] Water was observed to desorb molecularly at 148 K, in a single peak which increased in desorption temperature with increasing exposure. This peak could not be saturated and demonstrated a linear increase in peak area with increasing exposure.[12] The peak showed characteristics of zero-order desorption and was assigned to the sublimation of water ice with a desorption energy of 43.4 kJ mol^{-1}. A small percentage of water was also observed to desorb at ∼180 K. This was tentatively assigned to the desorption of intercalated water. A series of isothermal TPD experiments were performed for varying water exposures. These experiments confirmed the observation of zero-order desorption kinetics in bulk ice.[12]

Isothermal TPD experiments have also been carried out to investigate the crystallization kinetics of water on HOPG.[14,15]

* Corresponding author. E-mail: w.a.brown@ucl.ac.uk.

10.1021/jp0528111 CCC: $30.25
Published on Web 08/12/2005

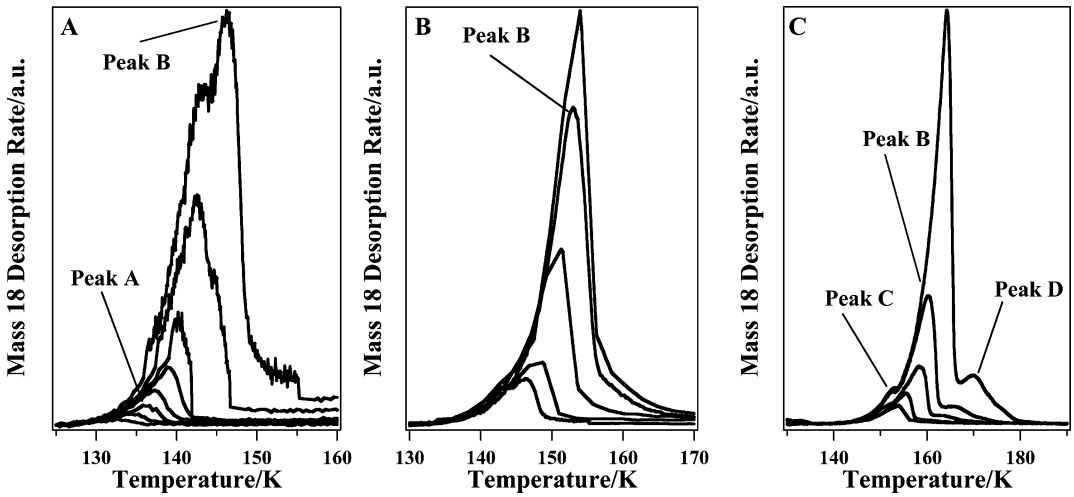

Figure 1. TPD spectra recorded following increasing exposures of water on an HOPG surface held at 92 K: (A) spectra recorded following doses of 0.04, 0.06, 0.1, 0.2, 0.3, 0.4, 1, and 2 langmuirs of water; (B) spectra recorded following doses of 2, 3, 7, 10, and 15 langmuirs of water; (C) spectra recorded following doses of 15, 20, 50, 100, and 275 langmuirs of water.

The structure of water adsorbed on a surface is highly dependent on the deposition conditions and the surface temperature. If deposition occurs below 135 K, ice grows as amorphous solid water (ASW),[16−18] with the exact morphology depending on the dosing conditions.[19,20] ASW has a glass transition temperature at ∼135 K,[21,22] above which it undergoes a phase transition to cubic crystalline ice (CI).[18,23] The phase transition has been reported to occur over a temperature interval from 130 to 160 K[15] and is accompanied by a reduction in vapor pressure, and hence desorption rate, by a factor of 3−100.[14,18,24] Isothermal TPD studies of water adsorbed on HOPG at ∼100 K[14,15] measured the transition of ASW to CI as a function of film thickness by monitoring the change in desorption rate associated with the transition. These studies showed that water does not wet the surface but instead forms three-dimensional (3D) droplets, which grow in size with increasing coverage.[15]

A density functional theory calculation has been performed by Sanfelix and co-workers to investigate the structure of water on a graphite (0001) surface.[25] This study showed that water molecules were physisorbed on the surface at all coverages. At low coverages, the water molecules showed little preference for orientation. However, as the coverage was increased, the water showed a preference for orientation of molecules such that the dipole was parallel to the surface. Further increases in coverage led to the formation of extended icelike layers.[25]

Here we present a detailed investigation of the adsorption of water on an HOPG surface at ∼90 K. RAIRS, TPD, and isothermal TPD studies have been used in parallel to allow a greater understanding of this adsorption system than has been obtained previously. Kinetic information, such as desorption orders, desorption energies, and preexponential factors, has also been determined from the TPD spectra. Detailed desorption orders and preexponential factors have not previously been determined for the desorption of water from an HOPG surface.

Methodology

Experiments were performed in an ultrahigh vacuum (UHV) chamber that has a base pressure of $\leq 2 \times 10^{-10}$ mbar. The HOPG sample was purchased from Goodfellows Ltd. and was cleaved prior to installation in the UHV chamber using the "Scotch Tape" method.[26] The sample was mounted by clamping, via tension wires, onto a piece of Ta foil which in turn was clamped on top of a piece of sapphire. Cooling of the sample was achieved by mounting the sapphire directly onto the end of a liquid nitrogen cooled coldfinger. Heating was achieved by passing current through W−Re heating wires which were spot welded to the Ta foil on which the HOPG was mounted. To ensure efficient heating of the HOPG, the sample had two grooves in the back of it, into which the heating wires fitted. These allowed the sample to be clamped snugly on top of the Ta foil/heating wire assembly. The temperature of the sample was monitored with an N-type thermocouple, also spot welded to the Ta foil directly behind the HOPG sample. Temperature control, during dosing and TPD experiments, was achieved via the use of a Eurotherm temperature controller coupled to Itools software. This allowed the temperature ramp during TPD experiments to be kept constant to within ± 0.01 K s^{-1}. The sample was cleaned before each experiment by annealing at 500 K in UHV for 3 min. Sample cleanliness was confirmed by the absence of any desorption during TPD experiments performed with no dosage. Water (distilled, deionized water) was admitted into the chamber by means of a high precision leak valve, and the purity was checked with a quadrupole mass spectrometer before each experiment and during dosing. All exposures are measured in langmuirs, where 1 langmuir $= 10^{-6}$ mbar s.

RAIR spectra were recorded using a Mattson Instruments RS1 research series Fourier transform infrared spectrometer coupled to a liquid nitrogen cooled MCT detector. All spectra were taken at a resolution of 4 cm^{-1} and are the result of the coaddition of 256 scans. In RAIRS experiments where the sample was heated, it was annealed to a predetermined temperature, held at this temperature for 3 min, and then cooled back down to the base temperature before a spectrum was recorded. TPD spectra were recorded with a Hiden Analytical HAL201 quadrupole mass spectrometer. All TPD spectra were recorded at a heating rate of 0.50 ± 0.01 K s^{-1}. This heating rate was chosen as it allowed a very constant heating rate to be maintained during the TPD experiments and it gave the best resolution between the different desorbing species observed in the TPD experiment. For isothermal TPD experiments, the sample was heated to 142 K at 0.50 ± 0.01 K s^{-1} and then held constant at that temperature until no further desorption was detected.

Results and Discussion

A. TPD Results. A series of TPD spectra for increasing exposures of water on HOPG at 92 K are shown in Figure 1.

At the lowest exposures, between 0.04 and 0.3 langmuirs, a single peak is observed, labeled as peak A. As the exposure is increased, this peak shifts up in temperature from approximately 132 to 138 K. Further increase in exposure leads to the appearance of a second peak, peak B, initially as a shoulder on peak A, at 146 K (Figure 1A). For a 2 langmuir exposure, peak B can clearly be distinguished from peak A and is the dominant species in the spectrum (Figure 1A). Increasing the exposure to 7 langmuirs and above leads to peak B dominating peak A until the two peaks can no longer be distinguished from each other (Figure 1B). This combined peak shifts up in desorption temperature with increasing exposure.

At the highest recorded exposures (Figure 1C), peak B continues to shift up in temperature with increasing exposure, with a desorption temperature of 164 K for a 275 langmuir exposure. This peak cannot be saturated and is the dominant feature in the desorption spectra seen in Figure 1C. Figure 1C shows two further desorption features labeled as peaks C and D. Peak C is observed as a distinctive bump on the low-temperature side of peak B, following exposures of 50 langmuirs and above. It is particularly prominent in spectra following exposures of 100 and 275 langmuirs and has a desorption temperature of 152 K. Similarly, peak D is observed following exposures of 50 langmuirs and above. This peak is initially observed as a high-temperature tail on peak B but is a distinct peak following exposures of 100 and 275 langmuirs. This peak increases in intensity and shifts to higher desorption temperatures as the exposure is increased. Once again this peak could not be saturated with increasing exposure.

It is possible to assign these desorption peaks by comparing the observed TPD spectra with previous studies of the adsorption of water. Previous studies of water adsorption on HOPG[12,13,27] have shown that water ice layers grow by a cluster growth mechanism. With this growth mode, island formation occurs. This results in water molecules being bonded in two different coordinations. Water molecules in the first two-dimensional (2D) layer, and on the edges of islands, have a lower coordination than molecules within the 3D islands. This difference in coordination leads to slightly different binding energies for water molecules, either in the first 2D layer and on the edges of islands or within the islands.[27] Therefore, peak A in Figure 1A is assigned to the desorption of water molecules from the 2D islands and/or from the edges of 3D islands. This assignment is confirmed by the observation of only peak A at the very lowest exposures of water on the HOPG surface.

Peak B is assigned to the desorption of water molecules from the surface of 3D islands, i.e., from multilayers of water. Water molecules on the surface of the islands are more highly coordinated than those on the edges of islands and would therefore be expected to have a higher desorption energy. This assignment is confirmed by the appearance of peak B at higher exposures than peak A. This is as expected, since the growth of 3D islands would be preceded by the formation of 2D islands. The assignment of peaks A and B to the desorption of water molecules from 2D and 3D islands respectively is in excellent agreement with a previous study of the adsorption of water on HOPG.[27]

As the exposure is increased, peaks A and B merge (Figure 1B). As the water layers grow, the proportion of low coordinated water molecules on island edges decreases with respect to the more highly coordinated molecules inside the islands. Hence peak B dominates peak A. The merging of the two peaks is assigned to the growth of water ice multilayers, confirming the assignment of peak B to the desorption of these multilayers. The assignment of peak B is further confirmed by the observed increase in desorption temperature with increasing exposure and by the fact that the peak cannot be saturated. This observation is also in agreement with previous studies.[28]

Peak C is observed as a bump on the low temperature side of peak B, at approximately 153 K, for high water exposures (Figure 1C). A similar feature has been observed at 150−160 K in previous studies of water adsorption on a variety of metal surfaces.[18,24,29,30] This has been assigned to an irreversible phase transition from ASW to CI. The phase transition is accompanied by a change in vapor pressure, and hence a change in the desorption rate, which manifests itself as a bump in the TPD spectrum. The phase transition from ASW to CI is a direct consequence of the temperature ramp applied during the TPD process. The phase transition is believed to occur for all exposures in which multilayers are present; however it can only be observed for exposures above 50 langmuirs using the experimental ramp rate (0.50 ± 0.01 K s^{-1}). For exposures below 50 langmuirs, the water adlayer is completely converted from ASW to CI in the time scale of the experiment and hence no bump is observed. Peak B (Figure 1) is therefore due to the desorption of crystalline water from HOPG. For exposures greater than 50 langmuirs, some desorption occurs from the residual ASW, which has not undergone a phase change in the time scale of the TPD experiment. Similar findings have been reported by Dohnalek and co-workers.[31] As previously shown,[32] it should be possible to observe the phase transition at lower exposures if a faster heating rate was used in the experiment. The phase transition from ASW to CI has not been observed in previous TPD studies of water adsorption on HOPG, as these studies involved films of water ice that were too thin for the transition to be observed.[12,27]

The appearance of peak D in Figure 1C has not previously been observed for the adsorption of water on HOPG. Peak D is only observed for exposures greater than 50 langmuirs and is therefore tentatively assigned to a further phase transition from CI to hexagonal ice, HI. HI is the only naturally found stable form of ice and is formed at a temperature of ∼200 K.[33] As for CI, HI is most likely formed as a result of the temperature ramp, applied in the TPD experiment.

B. RAIRS Results. To gain a clearer understanding of the adsorption of water on HOPG, RAIRS experiments were also performed. RAIR spectra following adsorption of water on HOPG at 100 K are shown in Figure 2. At low exposures, no vibrational bands are observed. This is in direct contrast to the TPD spectra shown in parts A and B of Figure 1, where desorption peaks are observed even at very low exposures. Following an exposure of 11 langmuirs, a broad band is observed centered at a frequency of ∼3405 cm^{-1} with a width of ∼280 cm^{-1} (Figure 2). As the exposure is increased, this band grows in intensity but does not undergo a frequency shift. Following an exposure of 50 langmuirs, this peak has broadened to approximately 450 cm^{-1} wide and appears to be developing into two peaks. This peak splitting is clearest in spectra following exposures of 100 and 300 langmuirs of water. A shallow shoulder is also observed at ∼3180 cm^{-1} for exposures greater than 100 langmuirs. Following a 300 langmuir exposure, the region between 3100 and 3600 cm^{-1} clearly shows three spectral features, as indicated in the bottom spectrum in Figure 2.

A second band is also observed at ∼1677 cm^{-1} for exposures above 100 langmuirs. This band is relatively low in intensity, but can clearly be seen in the spectrum recorded following a 300 langmuir exposure. A further increase in exposure leads to an increase in intensity of all bands but does not lead to the

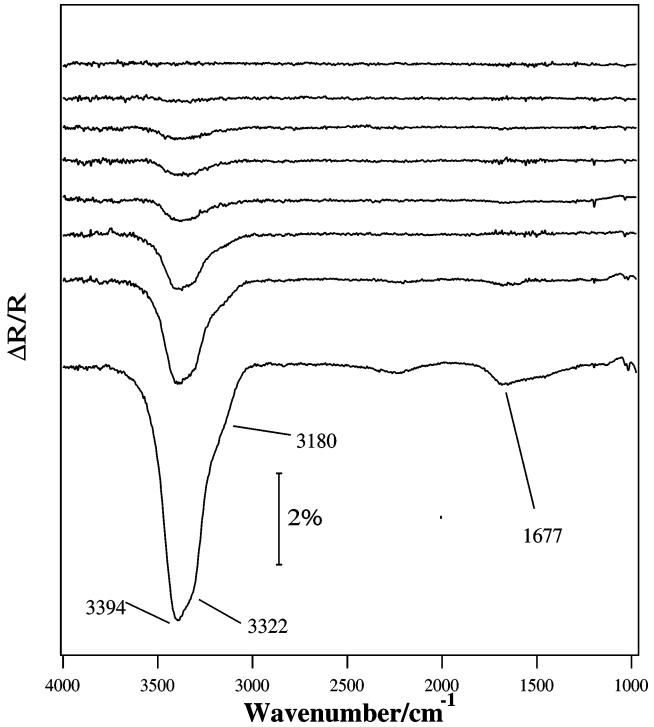

Figure 2. RAIR spectra recorded following water adsorption on HOPG at 100 K. The exposures of water were (top to bottom) 3, 5, 11, 15, 20, 50, 100, and 300 langmuirs.

observation of any additional features. No frequency shift is observed for any of the vibrational bands, nor is it possible to saturate any of the spectral features.

The bands observed in Figure 2 can be assigned confidently by comparing the observed frequencies with previous HREELS studies of water adsorbed on HOPG at similar temperatures.[11,12] The bands observed between 3100 and 3600 cm^{-1} are assigned to O−H stretching modes, and the band observed at 1677 cm^{-1} is assigned to the HOH scissors mode. The observed features are comparable to those recorded for multilayer water adsorbed on a variety of metal surfaces and for solid water.[9] Hence, the spectral features shown in Figure 2 are assigned to physisorbed multilayers of water ice. The multilayers of water are believed to exist in hydrogen bonded networks, as demonstrated by the broadness of the O−H stretching bands shown in Figure 2. Broad O−H stretching bands have previously been observed for hydrogen-bonded networks of water multilayers adsorbed on a variety of surfaces.[9,10]

The assignment of the vibrational features observed in Figure 2 to water multilayers is confirmed by the TPD spectra presented in Figure 1. The TPD spectra show that at comparable exposures (>11 langmuirs), the TPD peaks observed are due to the desorption of multilayers of water. Note that the island growth observed in the TPD spectra could not be observed in the RAIR spectra. Previous vibrational studies of island growth of water on HOPG[12,13] have followed the frequency shift of the frustrated rotational and translational modes. However, these modes are too low in frequency to be observed with the RAIRS setup used here.

It is possible to determine the phase of water present on the surface by monitoring the appearance of the O−H stretch.[34−36] The shape and structure of the vibrational band alters, depending on whether the water is ASW or CI in nature. The shape of the O−H stretch shown in the bottom spectrum in Figure 2 is in excellent agreement with previous spectra recorded of ASW on Cu{110}[35] and on Pt{533};[36] hence the water adlayer is assigned as ASW. Note that the TPD spectra shown in Figure 1 appear to contradict this assignment, since the majority of the adlayer desorbs as CI. However, this anomaly is explained by the TPD process itself, which converts the ASW to CI hence leading to the desorption of water mainly in the CI phase.

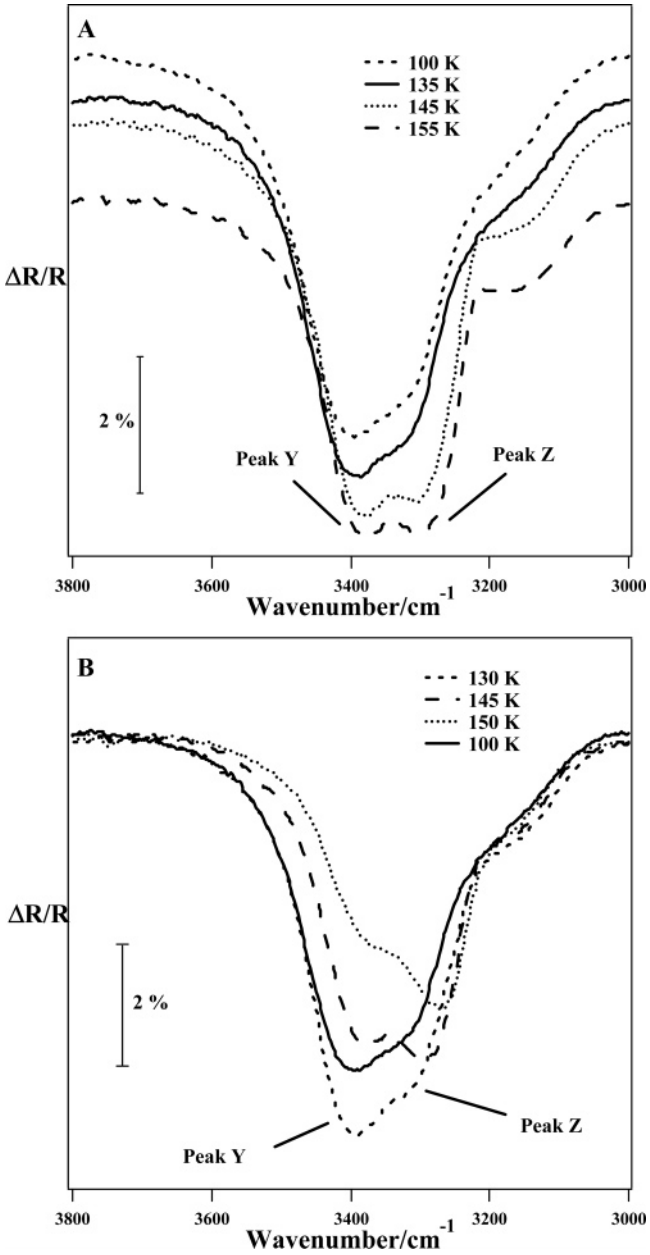

Figure 3. RAIR spectra showing the result of increasing the HOPG surface temperature on the O−H stretching region of the water spectrum: (A) the effect of annealing a multilayer of water (300 langmuirs exposure) adsorbed on HOPG at 100 K; (B) the effect of altering the adsorption temperature on a multilayer resulting from a 300 langmuir exposure of water on the HOPG surface.

To observe the phase change from ASW to CI with RAIRS, experiments were performed where multilayers of water adsorbed on HOPG were annealed to various temperatures. Annealing the adlayer causes a marked change in the appearance of the bands in the O−H stretching region (Figure 3A), and all bands disappear from the spectrum by 175 K, implying complete desorption of the water adlayer. This desorption temperature is in agreement with the desorption temperature observed in the TPD study.

Figure 3A shows a close up of the O−H stretching region of a series of RAIR spectra resulting from the annealing of a water

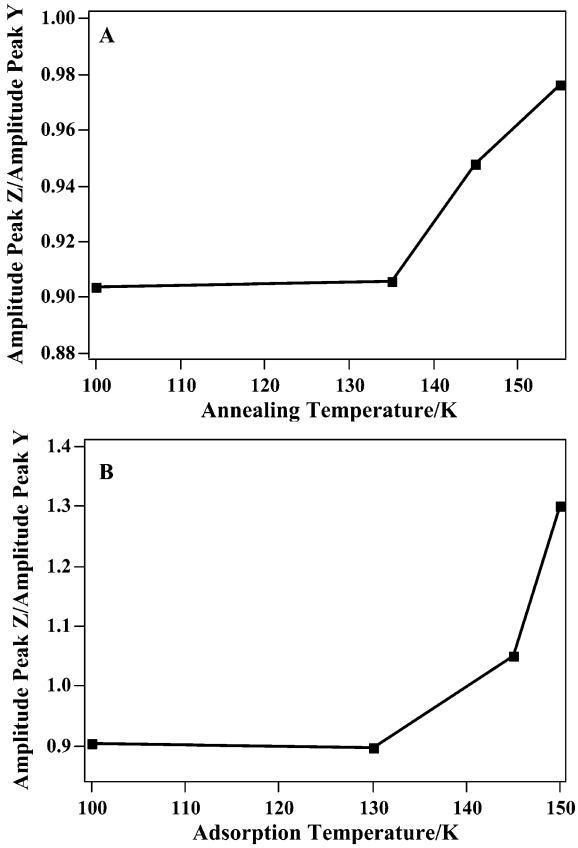

Figure 4. Graphs showing the effect of surface temperature on the ratio of the amplitudes of peak Z (3322 cm^{-1}) and peak Y (3394 cm^{-1}) observed in Figure 3: (A) the ratio of the amplitudes of these peaks as a function of annealing temperature; (B) the ratio of the peak amplitudes as a function of adsorption temperature.

adlayer (300 langmuirs exposure) to various temperatures. Annealing the adlayer from 100 to 155 K causes a marked change both in the shape and in the structure of the O−H stretching mode. This change in shape is also accompanied by a slight downshift (∼20 cm^{-1}) in frequency of the entire spectral feature. Annealing the adlayer to 135 K leads to the two peaks observed at 3394 cm^{-1} (peak Y) and 3322 cm^{-1} (peak Z) becoming more pronounced and distinct. Following both adsorption at 100 K and annealing to 135 K, peak Z has approximately 90% of the amplitude of peak Y. However, annealing to 145 K leads to a clear separation of the peaks and a change in the ratio of the amplitudes of the two peaks, so that the amplitude of peak Z is 94% of the amplitude of peak Y. This trend continues as the adlayer is annealed to 155 K, when the two peaks become almost comparable in amplitude, as shown in Figure 4A. Additionally, the low-frequency shoulder at 3180 cm^{-1} becomes more pronounced when the adlayer is annealed (Figure 3A). In agreement with previous observations,[36] it is proposed that the changes observed in the spectra shown in Figure 3A occur as a result of the conversion of ASW, adsorbed at 100 K, to CI.

To complement the annealing experiments, and to test this hypothesis further, RAIRS experiments were also carried out to determine the effect of adsorption temperature on the water layer adsorbed on HOPG. Figure 3B shows the RAIR spectra that result when the adsorption temperature of a 300 langmuirs exposure of water on HOPG is varied. Note that only the O−H stretching region is shown in Figure 3B. Figure 3B shows that the adsorption temperature has a marked effect on the shape and structure of the O−H stretch. An increase in adsorption temperature leads to a downshift in the frequency of the two peaks at 3394 cm^{-1} (peak Y) and 3322 cm^{-1} (peak Z) by approximately 40 cm^{-1}. Adsorption at 100 K leads to peak Z having an amplitude approximately 90% of that of peak Y. Adsorption at 130 K leads to a sharpening of the two features, but does not alter the ratio between the amplitudes of the two peaks (Figure 4B). Increasing the adsorption temperature to 145 K alters the amplitude ratio between peaks Y and Z so that peak Z has a larger amplitude than peak Y. Further increasing the adsorption temperature to 150 K sees a continuation of this trend, with peak Z now having an amplitude 30% greater than peak Y (Figure 4B). No change is observed in the low-frequency shoulder at 3180 cm^{-1} as a function of adsorption temperature.

As already discussed, water ice takes on an ASW structure below ∼130 K and a CI structure above ∼130 K. The changes observed in the spectra, shown in Figure 3, are therefore assigned to the phase transition from ASW to CI in the water adlayer. The spectra shown in Figure 3B are assigned as ASW, CI, or a combination of both, depending on the adsorption temperature. Adsorption at 100 K and at 130 K results in water taking on an ASW structure, while adsorption at 150 K results in a CI structure (Figure 3B). Adsorption at 145 K leads to a mixture of both. These assignments are confirmed by comparison with previous studies of the adsorption of water on metal surfaces as a function of adsorption temperature.[34−38] It is clear from the spectra shown in Figure 3B that it is possible to use the shape of the O−H stretching mode of water to identify the phase of the water. The spectrum recorded following adsorption at 150 K represents the fingerprint of pure CI and that recorded following adsorption at 100 K (or 130 K) represents the spectrum of pure ASW.

It is clear by comparing parts A and B of Figure 3 that annealing a water adlayer to a certain temperature does not lead to the same water structure as for adsorption at that temperature. This is in contrast to a previous study, where RAIR spectra obtained by dosing at a set temperature and those obtained by isothermal crystallization of ASW dosed at 100 K were identical.[36] The apparent disagreement between the study by Backus and co-workers[36] and this study can be explained by considering how the experiments in this study were performed. The spectra shown in Figure 3B were recorded following adsorption at a specified temperature with the sample held at that temperature throughout the adsorption process. In this manner the phase of the adlayer depends solely on the adsorption temperature. Hence the spectra shown in Figure 3B are a true reflection of which phase of water is present on the surface. Alternatively, the spectra shown in Figure 3A were recorded following adsorption at 100 K, heating the sample to the desired temperature, holding at that temperature for 3 min, and then allowing the sample to cool back down to 100 K. Hence, the phase of the adlayer is dependent on the temperature to which it was annealed and for how long it was annealed. For these experiments, adsorption at 100 K leads to the formation of ASW, and subsequent annealing to higher temperatures converts the ASW to CI. However, the spectra recorded following annealing to 145 and 155 K (Figure 3A) are believed to be indicative of a mixture of ASW and CI, rather than pure CI. This is a result of incomplete conversion of the ASW to CI during the annealing process. If the adlayer was annealed for longer, complete conversion from ASW to CI would occur at the higher temperatures and hence the spectra in Figure 3 would be identical.

C. Isothermal TPD Results. A series of isothermal TPD experiments were also carried out so that a clearer understanding of the ASW to CI phase transition could be gained. Water was initially adsorbed on the HOPG surface at 93 K. The sample

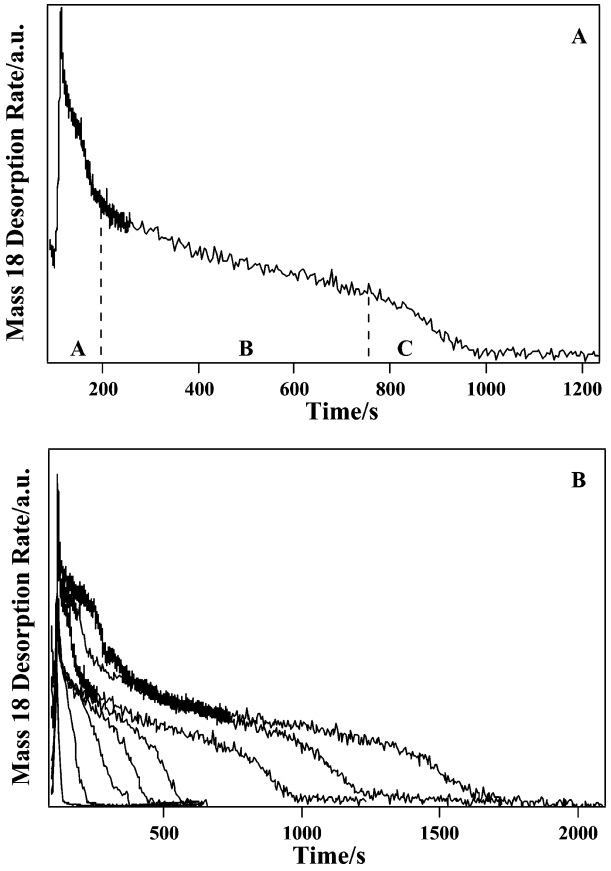

Figure 5. Isothermal TPD spectra recorded at 142 K following water adsorption on HOPG at 93 K: (A) an isothermal spectrum for desorption recorded following a 40 langmuir exposure of water, labeling of the regions of the spectrum is described in the text; (B) a series of isothermal TPD spectra for varying exposures of water on HOPG. The spectra are for exposures of water of 2.5, 6, 12.5, 20, 25, 40, 65, and 80 langmuirs.

was then annealed to 142 K at 0.50 ± 0.01 K s^{-1} and held at that temperature until the desorption signal from the QMS was comparable to the background signal. A temperature of 142 K was chosen in accordance with previous isothermal TPD studies of water on HOPG.[12,14,15] Figure 5A shows an isothermal TPD spectrum recorded following a 40 langmuir exposure of water on HOPG. The spectrum is divided into three regions, labeled A, B, and C. Initially there is an increase in the desorption rate as desorption of the adlayer takes place during both the initial temperature ramp and with the sample held at 142 K. The desorption rate then rapidly decreases. After approximately 190 s, the desorption rate slows considerably. This marks the end of region A. The desorption rate then decreases slowly until 760 s, when the desorption rate changes drastically again. The region between 190 and 760 s is labeled as region B. The final region of the spectrum, region C, signifies the final desorption of the remaining water adlayer.

It is possible to assign the three regions to different kinetic regimes by comparing Figure 5A with previous isothermal TPD studies of water on HOPG[14,15] and on single-crystal metal surfaces.[18] When water is adsorbed at 93 K the overlayer formed is ASW. In region A two thermodynamically driven, parallel, processes occur in the ASW,[15] namely, the desorption of the ASW film and the crystallization of ASW to CI. The initial high desorption rate observed in region A is a result of the high vapor pressure of the desorbing ASW compared to the CI. As crystallization occurs, the rate of desorption rapidly decreases until the adlayer has been completely transformed from ASW to CI. This is equivalent to the bump observed in the TPD spectra shown in Figure 1. Once the phase change has occurred, the rate of desorption levels out to an almost constant value (region B). Region B corresponds to the desorption of multilayers of the annealed adlayer, which are CI in structure. Note that, if desorption of the multilayer obeyed perfect zero-order kinetics, the desorption rate would be constant in region B and a plateau would be observed. It is clear from Figure 5A that this is not the case. This will be confirmed later when the desorption order of multilayers of water from the HOPG surface is calculated.

Region C indicates the kinetic region where the water adlayer does not cover the whole surface. In this region, islands of water ice alternate with bare areas of the HOPG surface.[14,15] Sublimation of the ice causes a monotonic decrease in island size and effective island surface area. This leads to the monotonic decrease in desorption rate observed in region C. Note that region B will only be observed if the water ice film is sufficiently thick for multilayers to form. If the ice film is not thick enough, region A will be followed directly by region C.

A series of isothermal TPD spectra for varying water exposures, and hence ice film thicknesses, are shown in Figure 5B. Figure 5B clearly shows that region A, the time taken for the ASW to crystallize, increases with increasing film thickness. Previous isothermal TPD studies of the adsorption of water on HOPG and on Pt{111} have shown that the time taken for crystallization becomes independent of film thickness for sufficiently thick films.[15] However, this was not observed for the adsorption of water on HOPG as shown in Figure 5B. Note that for low exposures ($\leq$6 langmuirs), region A is followed directly by region C. This implies that, for exposures $\leq$6 langmuirs, desorption of multilayers takes place simultaneously with the crystallization of the ASW. For exposures greater than 6 langmuirs, crystallization takes place before all of the multilayers have desorbed. Figure 5B also confirms that the desorption of water multilayers, region B, is not a perfect zero-order process as already seen in Figure 5A.

D. Quantitative Analysis of TPD Spectra. To acquire a better understanding of the desorption kinetics of water adsorbed on HOPG desorption orders, desorption energies and preexponential factors were calculated. These calculations use the TPD data shown in Figure 1. An attempt was made to separate the TPD spectra into contributions from peaks A−D using a fitting program; however the quality of the fits was insufficient. An attempt was also made to carry out analysis for peak A alone, but this led to spurious results due to an insufficient number of data points. Therefore analysis has only been carried out for the desorption of physisorbed crystalline water multilayers from HOPG (peak B in Figure 1). Note that exposures above 50 langmuirs were not used in the analysis. This is due to the phase transition from ASW to CI (peak C), and subsequently to HI (peak D), which affects the desorption rate and again leads to spurious results.

Uptake and Desorption Order. The signal intensity recorded by the mass spectrometer, $I(T)$, is proportional to the rate of change of coverage of the adsorbate. Therefore, the integrated area under each TPD spectrum is proportional to the coverage of adsorbate on the surface. In the experiments described here, it is not possible to measure the absolute coverage of the adsorbate. Hence the integrated area under each spectrum is proportional to the relative coverage of adsorbate on the surface. It is therefore possible to determine the uptake of water on HOPG as a function of exposure. A graph of the uptake of water on HOPG at 92 K (not shown) can be fitted with a single straight

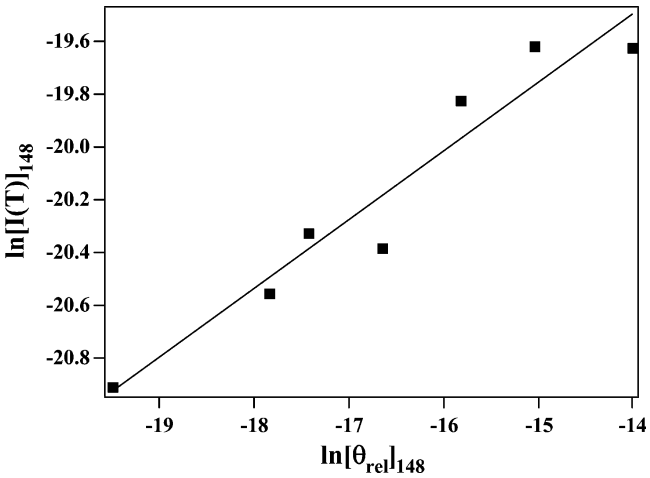

Figure 6. A plot of $\ln[I(T)]_{T_x}$ against $\ln[\theta_{rel}]_{T_x}$ for a fixed temperature, T_x, of 148 K for various exposures of water adsorbed on HOPG at 92 K. The gradient of this graph gives the order of desorption.

line with an R^2 value of 0.999, indicating a constant sticking probability for physisorbed water adsorbed on HOPG at 92 K, as expected.

Desorption orders for water adsorption on HOPG were calculated in an identical manner to those previously calculated for CH_3OH adsorption on HOPG.[39] The desorption order can be calculated using the Polanyi−Wigner equation[40]

$$r_{des} = -\frac{d\theta}{dt} = \upsilon_n \theta^n \exp\left[\frac{-E_{des}}{RT_s}\right] \quad (1)$$

where r_{des} is the rate of desorption, υ_n is the preexponential factor of the desorption process of order n, θ is the coverage, E_{des} is the desorption activation energy, R is the gas constant, and T_s is the surface temperature. Remembering that the rate of change of coverage with respect to time (which is proportional to the intensity of the measured TPD trace, $I(T)$) can be linked to the rate of change of coverage with respect to temperature and that only a relative coverage, θ_{rel}, can be obtained in the experiments described here, eq 1 becomes

$$I(T) \propto \upsilon_n \theta_{rel}{}^n \exp\left[\frac{-E_{des}}{RT_s}\right] \quad (2)$$

Rearranging and taking logarithms of this equation gives eq 3

$$\ln[I(T)] \propto n \ln[\upsilon_n \theta_{rel}] - \frac{E_{des}}{RT_s} \quad (3)$$

Desorption orders, and hence a confirmation of the peak assignments, can be obtained from eq 3 by plotting a graph of $\ln[I(T)]_{T_x}$ against $\ln[\theta_{rel}]_{T_x}$ at a fixed temperature, T_x. The gradient of such a plot is n, the order of desorption.[39] Note that, to perform this plot, it is assumed that the desorption energy and preexponential factor do not vary with coverage or temperature. The validity of these assumptions will be demonstrated later. Figure 6 shows a plot of $\ln[I(T)]_{T_x}$ against $\ln[\theta_{rel}]_{Tx}$ for a T_x value of 148 K for water adsorption on HOPG at 92 K. The graph has a gradient of 0.26 ± 0.03. The error in this gradient was obtained by determining the gradient of the best fit line and also of the lines with greatest and least slopes. Error bars are not shown on the graph in Figure 6 as they are too small to be observed on this scale. The desorption order calculation was repeated for a range of fixed temperatures and the gradients obtained from the plots, and hence the desorption order for multilayers of crystalline water ice adsorbed on HOPG are given in Table 1.

TABLE 1: Table Showing Calculated Desorption Orders for Multilayers of Water Ice Adsorbed on HOPG at 92 K

T_x/K	desorption order for multilayer water	T_x/K	desorption order for multilayer water
148	0.26 ± 0.03	156	0.23 ± 0.05
153	0.21 ± 0.02	158	0.25 ± 0.04

Table 1 shows that multilayers of water have an average desorption order of 0.24 ± 0.02. This fractional desorption order is in agreement with the isothermal TPD results presented in Figure 5, which show that the desorption of water does not obey zero-order kinetics. This fractional desorption order is attributed to the hydrogen-bonded network, which exists in the water multilayer, and ensures that desorption of one water molecule is not independent of the desorption of other molecules, as would be expected for zero-order desorption. Hydrogen-bonded systems have previously been shown to exhibit fractional order desorption kinetics.[39,41,42] Evidence for a hydrogen bonded network within the water adlayer has also been shown in the broadness of the observed O−H stretching bands presented in the RAIR spectra (Figure 2).

Further evidence for a non-zero-order desorption process arises from the TPD spectra themselves, shown in Figure 1. The spectra do not share leading edges, as is expected for perfect zero-order desorption. A previous TPD study of the adsorption of water on HOPG concluded a zero-order desorption process for multilayers of water from the TPD peak shape.[12] This is clearly in disagreement with the results presented here. However, no quantitative analysis was carried out with respect to desorption orders by Chakarov and co-workers.[12]

Desorption Energy. It is also possible to calculate the desorption energy for water multilayers adsorbed on HOPG. In this way it is possible to gain an indication of the binding strength within the water multilayer. The desorption energy has been calculated using the complete analysis technique,[40,43] a method which uses the family of desorption spectra shown in Figure 1B and is based on rigorous application of the Polanyi−Wigner equation (eq 1).[40,43] Rearrangement of eq 3 leads to

$$\ln I(T) \propto n \ln \upsilon_n + n \ln \theta_{rel} - \frac{E_{des}}{RT_s} \quad (4)$$

The essence of the method is that TPD traces are converted to give a plot of coverage against temperature. The relative coverage is then fixed at some chosen value θ_{rel}', and the corresponding temperatures are read off at that chosen value of θ_{rel}', across all exposures. As a result, the relative coverage across all exposures becomes constant and eq 4 becomes

$$\ln I(T) \propto n \ln \upsilon_n - \frac{E_{des}}{RT_s} \quad (5)$$

The temperatures for each exposure, at this fixed relative coverage value θ_{rel}', are then related to the corresponding desorption intensity, $I(T)$, for the family of TPD curves shown in Figure 1B. An Arrhenius plot of $\ln[I(T)]$ against $1/T$ for all exposures at θ_{rel}' then gives a straight line with a gradient of $-E_{des}/R$. The only assumptions made in this analysis are that the preexponential factor and the desorption energy do not vary with either coverage or temperature. As shown later, these are both valid assumptions in this case.

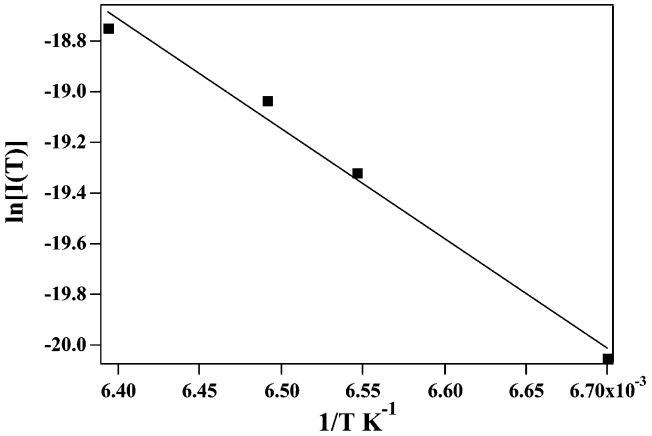

Figure 7. An Arrhenius plot of ln[$I(T)$] against $1/T$ for a fixed relative coverage value of 1.4×10^{-8} au. The gradient of the graph gives a desorption energy of 36.2 ± 2.1 kJ mol^{-1} for the desorption of multilayer water from HOPG.

TABLE 2: Table Showing Desorption Energies for Multilayer Water Adsorbed on HOPG for a Range of Fixed Relative Coverage Values[a]

fixed relative coverage value, θ_{rel}'/au	desorption energy/ kJ mol^{-1}	fixed relative coverage value, θ_{rel}'/au	desorption energy/ kJ mol^{-1}
1.4×10^{-8}	36.2 ± 2.1	2.2×10^{-8}	38.6 ± 1.6
1.8×10^{-8}	42.3 ± 1.4	2.35×10^{-8}	40.1 ± 1.2
2.0×10^{-8}	42.4 ± 1.9		

[a] These desorption energies were obtained using the complete analysis method.

Figure 7 shows an Arrhenius plot for a relative coverage of 1.4×10^{-8} a.u. The resulting desorption energy, obtained from the gradient of this graph, is 36.2 ± 2.1 kJ mol^{-1}. This process was repeated for several values of θ_{rel}' and Table 2 lists the desorption energies obtained. As for the desorption order, the error in the desorption energy was obtained by determining the gradient of the best fit line and also of the lines with greatest and least slopes. Error bars are again not shown on the graph in Figure 7 as they are too small to be observed on this scale. Table 2 shows good agreement between the calculated desorption energies for multilayers of water adsorbed on HOPG for a range of fixed relative coverages, confirming the assumption that E_{des} does not vary with coverage. From Table 2 an average value of 39.9 ± 0.8 kJ mol^{-1} is obtained for the desorption energy of crystalline water multilayers adsorbed on HOPG at 92 K. This corresponds to a strongly physisorbed or weakly chemisorbed adsorbate and is in excellent agreement with a previously reported value of 43.4 ± 2.9 kJ mol^{-1} for multilayers of water adsorbed on HOPG.[12] This desorption energy is also comparable to the sublimation enthalpy of ice, which has a reported value of 47.2 kJ mol^{-1}.[44] However, this desorption energy is smaller than that previously reported for the isothermal desorption of water from Ru{001}.[45]

Preexponential Factor. It is also possible to evaluate a preexponential factor for the desorption of water from HOPG. Along with the desorption order and desorption energy, these experimentally derived preexponential factors can then be incorporated into computational models of star-forming regions.[46,47] For the data shown here it is not possible to determine the preexponential factor directly from an Arrhenius plot such as that shown in Figure 7, since the absolute coverage of water on the surface is not known. However, it is possible to estimate the preexponential factor for water adsorbed on HOPG by converting the relative coverage and relative intensity into actual coverage and actual intensity, respectively. This can be achieved by estimating the exposure at which there are no bare patches left on the HOPG surface, i.e., approximate monolayer saturation. It is then possible to estimate the number of adsorbates present when saturation of the first adlayer is achieved. By using the fact that the sticking probability for water adsorption is constant, it is then possible to scale all relative coverages to absolute coverages.

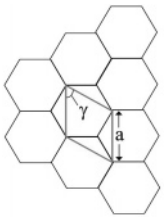

Figure 8. A schematic diagram showing the structure of the HOPG surface. Every corner of each hexagon represents a carbon atom. The unit cell is marked on the diagram, along with the lattice constant, a, and the corresponding unit cell angle, α.

Figure 8 shows the honeycomb structure of the HOPG surface. Each unit cell contains two atoms and has an area of 5.24×10^{-20} m^2. This gives a surface atom density for HOPG of 3.82×10^{19} atoms m^2. To calculate the number of adsorbates present on the surface, and hence estimate the coverage, a few approximations need to be made. By looking at the isothermal TPD spectra in Figure 5B, it is proposed that no bare patches are left on the HOPG surface for exposures greater than ~6 langmuirs. This is indicated by the lack of region B in isothermal TPD spectra recorded following exposures <6 langmuirs. An exposure of 7 langmuirs in Figure 1B is therefore approximated as a saturated first layer of water on HOPG. The validity of this assumption will be discussed later. The saturated first layer consists of an array of water molecules arranged in a hydrogen-bonded network. To estimate the number of molecules present in this layer, each water molecule is treated as a circle, with a radius corresponding to the O−H bond length. Each circle is then hydrogen bonded to other circles to form a two-dimensional array. To compute the surface area occupied by each circle, and hence each molecule, an O−H bond length of 0.957 Å and a hydrogen bond length of 1.97 Å are used.[44] This gives the area occupied by each water molecule as 2.69×10^{-19} m^2, and hence the number of adsorbates per unit area is 3.71×10^{18} molecules m^{-2}. The actual coverage, for a 7 langmuir exposure, is then given by this number divided by the HOPG surface density and is equal to ~0.1 monolayers.

As shown earlier, the uptake of water on HOPG is constant as a function of exposure; hence the number of adsorbates per unit area, as calculated above, can be directly related to the area under the 7 langmuir TPD curve. In this way a scaling factor can be used to convert all mass spectrometer intensities, and hence relative coverages, to actual coverages. The area under the 7 langmuir TPD curve (Figure 1B) is 2.36×10^{-8} au, which corresponds to an absolute coverage of 3.71×10^{18} molecules m^{-2}. Therefore all relative coverages have been scaled by a factor of 1.6×10^{26} to allow conversion to absolute coverage. This allows calculation of the preexponential factor for the adsorption of multilayers of water on HOPG. Rearrangement of eq 1 gives an expression for the preexponential factor υ_n

$$\upsilon_n = \frac{I(T)}{\theta^n \exp\left[\frac{-E_{des}}{RT_s}\right]} \tag{6}$$

TABLE 3: Table Showing the Effect of Altering the Exposure Corresponding to a 0.1 Monolayer Coverage, Which Equates to Saturation of the First Layer, on the Preexponential Factor for Water Adsorbed on HOPG at 92 K

exposure/ langmuir	preexponential factor[a]/molecules m^{-2} s^{-1}
3	9×10^{25}
7	4×10^{26}
15	3×10^{26}
20	2×10^{26}

[a] The units for the preexponential factor are those expected for zero-order desorption, despite the observation of a fractional desorption order.

TABLE 4: Table Showing the Effect of Altering the Desorption Order on the Preexponential Factor for Water Adsorbed on HOPG at 92 K[a]

desorption order	preexponential factor[b]/molecules m^{-2} s^{-1}
0.22	1×10^{27}
0.24	4×10^{26}
0.26	3×10^{26}

[a] It has been assumed that a 7 langmuir exposure is equivalent to a coverage of 0.1 monolayers. [b] The units for the preexponential factor are those expected for zero-order desorption, despite the observation of a fractional desorption order.

TABLE 5: Table Showing the Effect of Altering the Desorption Energy on the Preexponential Factor for Water Adsorbed on HOPG at 92 K[a]

desorption energy/kJ mol^{-1}	preexponential factor[b]/molecules m^{-2} s^{-1}
39.1	3×10^{26}
39.9	4×10^{26}
40.7	1×10^{27}

[a] It has been assumed that a 7 langmuir exposure is equivalent to a 0.1 monolayer coverage. [b] The units for the preexponential factor are those expected for zero order desorption, despite the observation of a fractional desorption order.

where $I(T)$ is the scaled mass spectrometer intensity signal, θ is the actual coverage derived from the scaled $I(T)$, n is the order of desorption calculated previously, and E_{des} is the desorption energy also calculated earlier. Using eq 6, it is possible to evaluate the preexponential factor at every recorded temperature point in every TPD trace. The average value is then evaluated for each exposure. This process was repeated for all TPD spectra for exposures between 7 and 20 langmuirs, and a further average value was obtained. No exposure dependence was noted for the calculated preexponential factors, confirming the earlier assumption that the preexponential factor is not a function of coverage.

To verify the validity of the assumptions made in the calculation of the preexponential factor, several checks were carried out. A possible source of error is the assumption that the saturation of a complete layer of water occurs for a 7 langmuir exposure, which corresponds to a coverage of 0.1 monolayers. To test this assumption, a 0.1 monolayer coverage was assumed to have been formed for a variety of exposures from 3 to 20 langmuirs. The outcome of this variation is shown in Table 3. To further test the assumptions made above, the errors associated with the desorption orders and the desorption energies calculated earlier were propagated through the calculations outlined above. The outcome of the errors associated with the order and desorption energy is shown in Tables 4 and 5.

Tables 3−5 show that the preexponential factor for multilayer desorption of water from HOPG has a value which ranges from 9×10^{25} molecules m^{-2} s^{-1} to 1×10^{27} molecules m^{-2} s^{-1}. The largest sources of error clearly arise from the propagation of errors in the desorption order and desorption energy. The estimate of the exposure at which saturation takes place is, surprisingly, the smallest source of error in the calculation, as shown in Table 3. This lack of sensitivity to the coverage is reassuring since TPD data point to the growth of irregular islands in the water adlayer rather than regular multilayers. This preexponential factor is in disagreement with a previous study of the adsorption of water on a gold substrate at 10 K, which calculated a preexponential factor of $10^{30} \pm 2$ molecules cm^{-2} s^{-1},[48] and with a study of the isothermal desorption of water from Ru{001}.[45] However, both previous studies[45,48] assumed that water desorption followed perfect zero-order desorption kinetics, which is clearly not the case here.

Summary and Conclusions

A detailed RAIRS and TPD study of the adsorption of water on HOPG at temperatures below 100 K has been performed. RAIRS experiments show that water is physisorbed on HOPG at all coverages. Experiments at higher surface temperatures show marked changes in the O−H stretching region of the infrared spectrum, which can be attributed to a phase transition from amorphous to crystalline water ice. The infrared signature of both phases of solid water on HOPG has been determined and can be used to identify the phase of the ice spectroscopically. The ability to distinguish between ice phases spectroscopically is especially important in the ISM, where water ice acts as a catalytic surface for the formation of many molecules.[49,50]

TPD spectra show the desorption of physisorbed water at all exposures. At very low coverages it is possible to distinguish the desorption of water molecules from 2D and 3D islands. The observation of island formation shows that water does not wet the HOPG surface and instead grows as hydrogen bonded clusters on the surface. As the water coverage on the surface increases, the desorption of multilayers of water dominates the spectrum. At very high exposures, the ASW to CI phase transition is observed as a bump in the TPD spectrum on the low-temperature side of the main desorption peak. The CI to HI phase transition can also be observed as a separate peak at 175 K. Neither of these phase transitions was observed in previous TPD investigations of water desorption from HOPG.[12,27,51]

Isothermal TPD spectra also show the ASW to CI phase transition, which is signaled by a rapid change in desorption rate. Isothermal spectra show that, in contrast to previous studies of water desorption from HOPG,[12] perfect zero-order desorption kinetics are not observed. Calculation of the desorption order from the recorded TPD spectra gives a value of 0.26 ± 0.02, which confirms this observation. This value of desorption order is in marked contrast to previous studies of water desorption from both HOPG[12] and Au surfaces,[4] where a desorption order of zero was assumed from the shape of the TPD spectra. The TPD data have also been used to determine the desorption energy, which has a value of 39.9 ± 0.8 kJ mol^{-1}, and the preexponential factor, which has a value ranging from 9×10^{25} to 1×10^{27} molecules m^{-2} s^{-1}. Both of these kinetic parameters are within the range expected for the desorption of a physisorbed species. Kinetic parameters for water desorption from HOPG have not previously been determined, despite their importance for the development of accurate models of the chemistry of the ISM. The desorption of water ice from grain surfaces is particularly relevant to the chemistry of so-called Hot Core regions,[46] where thermal desorption processes readily occur. In the past, astronomers have assumed that the desorption of all

species found in interstellar ices occurs simultaneously. However, recent work[46] has shown that this is not the case and that accurate kinetic parameters concerning thermal desorption are essential to allow a detailed understanding of the chemistry of Hot Cores to be obtained. Data from the studies described here will be incorporated into appropriate astronomical models[47] to investigate the effect of the kinetic parameters on the desorption of species found in interstellar ices. In particular, these investigations will focus on the role that the nature of the surface plays in the chemistry of the ISM. The results of previous studies,[46] investigating the desorption of model ices from a Au surface, will be compared with our data for desorption from HOPG, a model dust grain surface.

Acknowledgment. The UK EPSRC are gratefully acknowledged for studentships for A.S.B. and A.J.W. and also for an equipment and consumables grant (GR/S15273/01).

References and Notes

(1) Williams, D. A. In *Dust and Chemistry in Astronomy*; Millar, T. J., Williams, D. A., Eds.; Institute of Physics Publishing: Bristol, 1993.
(2) Whittet, D. C. B. Observations of Molecular Ices. In *Dust and Chemistry in Astronomy*; Millar, T. J., Williams, D. A., Eds.; Institute of Physics Publishing: Bristol, 1993; p 9.
(3) Whittet, D. C. B. *Dust in the Galactic Environment*; Institute of Physics Publishing: Bristol, 2003.
(4) Collings, M. P.; Anderson, M. A.; Chen, R.; Dever, J. W.; Viti, S.; Williams, D. A.; McCoustra, M. R. S. *Mon. Not. R. Astron. Soc.* **2004**, *354*, 1133.
(5) Perry, J. S. A.; Price, S. D. *Astrophys. Space Sci.* **2003**, *285*, 769.
(6) Pirronello, V.; Liu, C.; Roser, J. E.; Vidali, G. *Astron. Astrophys.* **1999**, *344*, 681.
(7) Perry, J. S. A.; Gingell, J. M.; Newson, K. A.; To, J.; Watanabe, N.; Price, S. D. *Meas. Sci. Technol.* **2002**, *13*, 1414.
(8) Katz, N.; Furman, I.; Biham, O.; Pirronello, V.; Vidali, G. *Astrophys. J.* **1999**, *522*, 305.
(9) Henderson, M. A. *Surf. Sci. Rep.* **2002**, *46*, 5.
(10) Thiel, P. A.; Madey, T. E. *Surf. Sci. Rep.* **1987**, *7*, 211.
(11) Phelps, R. B.; Kesmodel, L. L.; Kelley, R. J. *Surf. Sci.* **1995**, *340*, 134.
(12) Chakarov, D. V.; Osterlund, L.; Kasemo, B. *Vacuum* **1995**, *46*, 1109.
(13) Chakarov, D. V.; Osterlund, L.; Kasemo, B. *Langmuir* **1995**, *11*, 1201.
(14) Lofgren, P.; Ahlstrom, P.; Chakarov, D. V.; Lausma, J.; Kasemo, B. *Surf. Sci.* **1996**, *367*, L19.
(15) Lofgren, P.; Ahlstrom, P.; Lausma, J.; Kasemo, B.; Chakarov, D. *Langmuir* **2003**, *19*, 265.
(16) Johari, G. P.; Hallbrucker, A.; Mayer, E. *J. Chem. Phys.* **1991**, *95*, 2955.
(17) Jenniskens, P.; Blake, D. F. *Science* **1994**, *265*, 753.
(18) Smith, R. S.; Huang, C.; Wong, E. K. L.; Kay, B. D. *Surf. Sci.* **1996**, *367*, L13.
(19) Stevenson, K. P.; Kimmel, G. A.; Dohnalek, Z.; Smith, R. S.; Kay, B. D. *Science* **1999**, *283*, 1505.
(20) Mayer, E.; Pletzer, R. *Nature* **1986**, *319*, 298.
(21) Hallbrucker, A.; Mayer, E.; Johari, G. P. *J. Phys. Chem.* **1989**, *93*, 4986.
(22) Handa, Y. P.; Klug, D. D. *J. Phys. Chem.* **1988**, *92*, 3323.
(23) Smith, R. S.; Kay, B. D. *Nature* **1999**, *398*, 788.
(24) Smith, R. S.; Kay, B. D. *Surf. Rev. Lett.* **1997**, *4*, 781.
(25) Sanfelix, P. C.; Holloway, S.; Kolasinski, K. W.; Darling, G. R. *Surf. Sci.* **2003**, *532*, 166.
(26) Wiesendanger, R.; Eng, L.; Hidber, H. R.; Oelhafen, P.; Rosenthaler, L.; Staufer, U.; Guntherodt, H. J. *Surf. Sci.* **1987**, *189*, 24.
(27) Chakarov, D.; Kasemo, B. *Phys. Rev. Lett.* **1998**, *81*, 5181.
(28) Kay, B. D.; Lykke, K. R.; Creighton, J. R.; Ward, S. J. *J. Chem. Phys.* **1989**, *91*, 5120.
(29) Speedy, R. J.; Debenedetti, P. G.; Smith, R. S.; Huang, C.; Kay, B. D. *J. Chem. Phys.* **1996**, *105*, 240.
(30) Dohnalek, Z.; Ciolli, R. L.; Kimmel, G. A.; Stevenson, K. P.; Smith, R. S.; Kay, B. D. *J. Chem. Phys.* **1999**, *110*, 5489.
(31) Dohnalek, Z.; Kimmel, G. A.; Ciolli, R. L.; Stevenson, K. P.; Smith, R. S.; Kay, B. D. *J. Chem. Phys.* **2000**, *112*, 5932.
(32) Smith, R. S.; Huang, C.; Wong, E. K. L.; Kay, B. D. *Phys. Rev. Lett.* **1997**, *79*, 909.
(33) Petrenko, V.; Whitworth, R. *Physics of Ice*; Oxford University Press: Oxford, 1999.
(34) Schaff, J. E.; Roberts, J. T. *J. Phys. Chem.* **1996**, *100*, 14151.
(35) Bensebaa, F.; Ellis, T. H. *Prog. Surf. Sci.* **1995**, *50*, 173.
(36) Backus, E. H. G.; Grecea, M. L.; Kleyn, A. W.; Bonn, M. *Phys. Rev. Lett.* **2004**, *92*, 236101.
(37) Nuzzo, R. G.; Zegarski, B. R.; Korenic, E. M.; Dubois, L. H. *J. Phys. Chem.* **1992**, *96*, 1355.
(38) Schaff, J. E.; Roberts, J. T. *J. Phys. Chem.* **1994**, *98*, 6900.
(39) Bolina, A. S.; Wolff, A. J.; Brown, W. A. *J. Chem. Phys.* **2005**, *122*, 044713.
(40) de Jong, A. M.; Niemantsverdriet, J. W. *Surf. Sci.* **1990**, *233*, 355.
(41) Wu, M.; Truoung, C. M.; Goodman, D. W. *J. Phys. Chem.* **1993**, *97*, 9425.
(42) Nishimura, S. Y.; Gibbons, R. F.; Tro, N. J. *J. Phys. Chem. B* **1998**, *102*, 6831.
(43) Kolasinski, K. W. *Surface Science*: *Foundations of Catalysis and Nanoscience*; John Wiley and Sons Ltd.: New York, 2002.
(44) Eisenberg, D.; Kauzmann, W. *The Structure and Properties of Water*; Oxford University Press: London, 1969.
(45) Smith, J. A.; Livingston, F. E.; George, S. M. *J. Phys. Chem. B* **2003**, *107*, 3871.
(46) Viti, S.; Collings, M. P.; Dever, J. W.; McCoustra, M. R. S.; Williams, D. A. *Mon. Not. R. Astron. Soc.* **2004**, *354*, 1141.
(47) Bolina, A. S.; Brown, W. A.; Viti, S. In preparation.
(48) Fraser, H. J.; Collings, M. P.; McCoustra, M. R. S.; Williams, D. A. *Mon. Not. R. Astron. Soc.* **2001**, *327*, 1165.
(49) Ehrenfreund, P.; Irvine, W.; Becker, L.; Blank, J.; Brucato, J. R.; Colangeli, L.; Derenne, S.; Despois, D.; Dutrey, A.; Fraaije, H.; Lazcano, A.; Owen, T.; Robert, F. *Rep. Prog. Phys.* **2002**, *65*, 1427.
(50) Ehrenfreund, P.; Fraser, H. J.; Blum, J.; Cartwright, J. H. E.; Garcia-Ruiz, J. M.; Hadamcik, E.; Levasseur-Regourd, A. C.; Price, S.; Prodi, F.; Sarkissian, A. *Planet. Space Sci.* **2003**, *51*, 473.
(51) Chakarov, D. V.; Gleeson, M. A.; Kasemo, B. *J. Chem. Phys.* **2001**, *115*, 9477.